

Study of scalar meson $a_0(1450)$ from $B \rightarrow a_0(1450)K^*$ Decays

Zhi-Qing Zhang *

*Department of Physics, Henan University of Technology,
Zhengzhou, Henan 450052, P.R.China*

(Dated: October 24, 2018)

Abstract

In the two-quark model supposition for the meson $a_0(1450)$, which can be viewed as either the first excited state (scenario I) or the lowest lying state (scenario II), the branching ratios and the direct CP-violating asymmetries for decays $B^- \rightarrow a_0^0(1450)K^{*-}$, $a_0^-(1450)K^{*0}$ and $\bar{B}^0 \rightarrow a_0^+(1450)K^{*-}$, $a_0^0(1450)\bar{K}^{*0}$ are studied by employing the perturbative QCD factorization approach. We find the following results: (a) For the decays $B^- \rightarrow a_0^-(1450)K^{*0}$, $\bar{B}^0 \rightarrow a_0^+(1450)K^{*-}$, $a_0^0(1450)\bar{K}^{*0}$, their branching ratios in scenario II are larger than those in scenario I about one order. So it is easy for the experiments to differentiate between the scenario I and II for the meson $a_0(1450)$. (b) For the decay $B^- \rightarrow a_0^0(1450)K^{*-}$, due to not receiving the enhancement from the K^* -emission factorizable diagrams, its penguin operator contributions are the smallest in scenario II, which makes its branching ratio drop into the order of 10^{-6} . Even so, its branching ratio in scenario II is still larger than that in scenario I about 2.5 times. (c) Even though our predictions are much larger than those from the QCD factorization results, they are still consistent with each other within the large theoretical errors from the annihilation diagrams. (d) We predict the direct CP- violating asymmetry of the decay $B^- \rightarrow a_0^-(1450)K^{*0}$ is small and only a few percent.

PACS numbers: 13.25.Hw, 12.38.Bx, 14.40.Nd

arXiv:1106.0368v1 [hep-ph] 2 Jun 2011

* Electronic address: zhangzhiqing@haut.edu.cn

I. INTRODUCTION

Along with many scalar mesons found in experiments, more and more efforts have been made to study the scalar meson spectrum theoretically [1–7]. Unlike the pseudoscalar, vector, axial, and tensor mesons constant of light quarks, which are reasonable in terms of their $SU(3)$ classification and quark content, the scalar mesons are too many to accommodate them in one nonet. In fact, the number of the current experimentally known scalar mesons is more than 2 times that of a nonet. So it is believed that there are at least two nonets below and above 1 GeV. Today, it is still a difficult but interesting topic. Our most important task is to uncover the mysterious structure of the scalar mesons. There are two typical schemes for the classification to them [1, 2]. Scenario I (SI): the nonet mesons below 1 GeV, including $f_0(600)$, $f_0(980)$, $K^*(800)$ and $a_0(980)$, are usually viewed as the lowest lying $q\bar{q}$ states, while the nonet ones near 1.5 GeV, including $f_0(1370)$, $f_0(1500)/f_0(1710)$, $K^*(1430)$, and $a_0(1450)$, are suggested as the first excited states. In scenario II (SII), the nonet mesons near 1.5 GeV are treated as $q\bar{q}$ ground states, while the nonet mesons below 1 GeV are exotic states beyond the quark model, such as four-quark bound states. It should be four scalar mesons in each nonet, but there are five nonet mesons near 1.5 GeV. People generally believe that $K_0^*(1430)$, $a_0(1450)$ and two isosinglet scalar mesons compose one nonet, it means that one of the three isosinglet scalars $f_0(1370)$, $f_0(1500)$, $f_0(1710)$ can not be explained as $q\bar{q}$ state and might be a scalar glueball. There are many discussions [8–11] which one is most possible a scalar glueball based on a flavor-mixing scheme for these three scalar mesons, which induces there are more ambiguous about their inner structures. By contrast, the scalar mesons $K_0^*(1430)$, $a_0(1450)$ have been confirmed to a conventional $q\bar{q}$ meson in many approaches [12–15]. So the calculations for the B decays involved in either of these two scalar mesons in the final states should be more trustworthy.

The production of the scalar mesons from B-meson decays provides a different unique insight to the inner structures of these mesons. It provides various factorization approaches a new usefulness. Here we would like to use the perturbative QCD (PQCD) approach to study $a_0(1450)$ in decays $B^- \rightarrow a_0^0(1450)K^{*-}$, $a_0^-(1450)\bar{K}^{*0}$ and $\bar{B}^0 \rightarrow a_0^+(1450)K^{*-}$, $a_0^0(1450)\bar{K}^{*0}$. Certainly, these decays have been studied within the QCD factorization approach [16], in which the factorizable annihilation diagrams are calculated through a phenomenological parameter. So there are large theoretical errors for the QCD factorization predictions. To make precise predictions of their branching ratios and CP-violating asymmetries, it is necessary to make reliable calculations for the contributions from the factorizable annihilation diagrams. By contrast, these diagrams are calculable within the PQCD approach effectively.

In the following, $a_0(1450)$ is denoted as a_0 in some places for convenience. The layout of this paper is as follows. In Sec. II, the relevant decay constants and light-cone distribution amplitudes of relevant mesons are introduced. In Sec. III, we then analyze these decay channels using the PQCD approach. The numerical results and the discussions are given in Sec. IV. The conclusions are presented in the final part.

II. DECAY CONSTANTS AND DISTRIBUTION AMPLITUDES

For the wave function of the heavy B meson, we take

$$\Phi_B(x, b) = \frac{1}{\sqrt{2N_c}}(\not{P}_B + m_B)\gamma_5\phi_B(x, b). \quad (1)$$

Here only the contribution of Lorentz structure $\phi_B(x, b)$ is taken into account, since the contribution of the second Lorentz structure $\bar{\phi}_B$ is numerically small [17] and has been neglected. For the distribution amplitude $\phi_B(x, b)$ in Eq.(1), we adopt the following model:

$$\phi_B(x, b) = N_B x^2(1-x)^2 \exp\left[-\frac{M_B^2 x^2}{2\omega_b^2} - \frac{1}{2}(\omega_b b)^2\right], \quad (2)$$

where ω_b is a free parameter, we take $\omega_b = 0.4 \pm 0.04$ Gev in numerical calculations, and $N_B = 91.745$ is the normalization factor for $\omega_b = 0.4$.

In the two-quark picture, the vector decay constant f_{a_0} and the scalar decay constant \bar{f}_{a_0} for the scalar meson a_0 can be defined as

$$\langle a_0(p) | \bar{q}_2 \gamma_\mu q_1 | 0 \rangle = f_{a_0} p_\mu, \quad (3)$$

$$\langle a_0(p) | \bar{q}_2 q_1 | 0 \rangle = m_{a_0} \bar{f}_{a_0}, \quad (4)$$

where $m_{a_0}(p)$ is the mass (momentum) of the scalar meson $a_0(1450)$. The relation between f_{a_0} and \bar{f}_{a_0} is

$$\frac{m_{a_0}}{m_2(\mu) - m_1(\mu)} f_{a_0} = \bar{f}_{a_0}, \quad (5)$$

where $m_{1,2}$ are the running current quark masses. For the scalar meson $a_0(1450)$, f_{a_0} will get a very small value after the $SU(3)$ symmetry breaking is considered. The light-cone distribution amplitudes for the scalar meson $a_0(1450)$ can be written as

$$\begin{aligned} \langle a_0(p) | \bar{q}_1(z)_l q_2(0)_j | 0 \rangle &= \frac{1}{\sqrt{2N_c}} \int_0^1 dx e^{ixp \cdot z} \\ &\times \{ \not{p} \Phi_{a_0}(x) + m_{a_0} \Phi_{a_0}^S(x) + m_{a_0} (\not{n}_+ \not{n}_- - 1) \Phi_{a_0}^T(x) \}_{jl}. \end{aligned} \quad (6)$$

Here n_+ and n_- are lightlike vectors: $n_+ = (1, 0, 0_T)$, $n_- = (0, 1, 0_T)$, and n_+ is parallel with the moving direction of the scalar meson. The normalization can be related to the decay constants:

$$\int_0^1 dx \Phi_{a_0}(x) = \int_0^1 dx \Phi_{a_0}^T(x) = 0, \quad \int_0^1 dx \Phi_{a_0}^S(x) = \frac{\bar{f}_{a_0}}{2\sqrt{2N_c}}. \quad (7)$$

The twist-2 light-cone distribution amplitude Φ_{a_0} can be expanded in the Gegenbauer polynomials:

$$\Phi_{a_0}(x, \mu) = \frac{\bar{f}_{a_0}(\mu)}{2\sqrt{2N_c}} 6x(1-x) \left[B_0(\mu) + \sum_{m=1}^{\infty} B_m(\mu) C_m^{3/2}(2x-1) \right], \quad (8)$$

where the decay constants and the Gegenbauer moments B_1, B_3 of distribution amplitudes for $a_0(1450)$ have been calculated in the QCD sum rules [18]. These values are all scale dependent and specified below:

$$\text{scenarioI} : B_1 = 0.89 \pm 0.20, B_3 = -1.38 \pm 0.18, \bar{f}_{a_0} = -(280 \pm 30)\text{MeV}, \quad (9)$$

$$\text{scenarioII} : B_1 = -0.58 \pm 0.12, B_3 = -0.49 \pm 0.15, \bar{f}_{a_0} = (460 \pm 50)\text{MeV}, \quad (10)$$

which are taken by fixing the scale at 1GeV.

As for the twist-3 distribution amplitudes $\Phi_{a_0}^S$ and $\Phi_{a_0}^T$, we adopt the asymptotic form:

$$\Phi_{a_0}^S = \frac{1}{2\sqrt{2N_c}} \bar{f}_{a_0}, \quad \Phi_{a_0}^T = \frac{1}{2\sqrt{2N_c}} \bar{f}_{a_0} (1 - 2x). \quad (11)$$

For our considered decays, the vector meson K^* is longitudinally polarized. The longitudinal polarized component of the wave function is given as

$$\Phi_{K^*} = \frac{1}{\sqrt{2N_c}} \{ \not{\epsilon} [m_{K^*} \Phi_{K^*}(x) + \not{p}_{K^*} \Phi_{K^*}^t(x)] + m_{K^*} \Phi_{K^*}^s(x) \}, \quad (12)$$

where the first term is the leading twist wave function (twist-2), while the second and third term are subleading twist (twist-3) wave functions. They can be parameterized as

$$\Phi_{K^*}(x) = \frac{f_{K^*}}{2\sqrt{2N_c}} 6x(1-x) \left[1 + a_{1K^*} C_1^{3/2}(2x-1) + a_{2K^*} C_2^{3/2}(2x-1) \right], \quad (13)$$

$$\Phi_{K^*}^t(x) = \frac{3f_{K^*}^T}{2\sqrt{2N_c}} (1-2x), \quad \Phi_{K^*}^s(x) = \frac{3f_{K^*}^T}{2\sqrt{2N_c}} (2x-1)^2, \quad (14)$$

where the longitudinal decay constant $f_{K^*} = (217 \pm 5)\text{MeV}$ and the transverse decay constant $f_{K^*}^T = (185 \pm 10)\text{MeV}$, the Gegenbauer moments $a_{1K^*} = 0.03, a_{2K^*} = 0.11$ [19] and the Gegenbauer polynomials $C_n^\nu(t)$ are given as

$$C_1^{3/2}(t) = 3t, \quad C_2^{3/2}(t) = \frac{3}{2}(5t^2 - 1). \quad (15)$$

III. THE PERTURBATIVE QCD CALCULATION

Under the two-quark model for the scalar meson $a_0(1450)$ supposition, the decay amplitude for $B \rightarrow a_0 K^*$ can be conceptually written as the convolution,

$$\mathcal{A}(B \rightarrow K^* a_0) \sim \int d^4 k_1 d^4 k_2 d^4 k_3 \text{Tr} [C(t) \Phi_B(k_1) \Phi_{K^*}(k_2) \Phi_{a_0}(k_3) H(k_1, k_2, k_3, t)], \quad (16)$$

where k_i 's are momenta of the antiquarks included in each meson, and Tr denotes the trace over Dirac and color indices. $C(t)$ is the Wilson coefficient which results from the radiative corrections at a short distance. In the above convolution, $C(t)$ includes the harder dynamics at a larger scale than the M_B scale and describes the evolution of local 4-Fermi operators from m_W (the W boson mass) down to the $t \sim \mathcal{O}(\sqrt{\Lambda M_B})$ scale,

where $\bar{\Lambda} \equiv M_B - m_b$. The function $H(k_1, k_2, k_3, t)$ describes the four-quark operator and the spectator quark connected by a hard gluon, whose q^2 is in the order of $\bar{\Lambda}M_B$ and includes the $\mathcal{O}(\sqrt{\bar{\Lambda}M_B})$ hard dynamics. Therefore, this hard part H can be perturbatively calculated. The function $\Phi_{(B, K^*, a_0)}$ are the wave functions of the vector mesons B, K^* and the scalar meson a_0 , respectively.

Since the b quark is rather heavy, we consider the B meson at rest for simplicity. It is convenient to use the light-cone coordinate (p^+, p^-, \mathbf{p}_T) to describe the meson's momenta,

$$p^\pm = \frac{1}{\sqrt{2}}(p^0 \pm p^3), \quad \text{and} \quad \mathbf{p}_T = (p^1, p^2). \quad (17)$$

Using these coordinates, the B meson and the two final state meson momenta can be written as

$$P_B = \frac{M_B}{\sqrt{2}}(1, 1, \mathbf{0}_T), \quad P_2 = \frac{M_B}{\sqrt{2}}(1 - r_{a_0}^2, r_{K^*}^2, \mathbf{0}_T), \quad P_3 = \frac{M_B}{\sqrt{2}}(r_{a_0}^2, 1 - r_{K^*}^2, \mathbf{0}_T), \quad (18)$$

respectively, where the ratio $r_{a_0(K^*)} = m_{a_0(K^*)}/M_B$, and $m_{a_0(K^*)}$ is the scalar meson a_0 (the vector meson K^*) mass. Putting the antiquark momenta in B, K^* , and a_0 mesons as k_1, k_2 , and k_3 , respectively, we can choose

$$k_1 = (x_1 P_1^+, 0, \mathbf{k}_{1T}), \quad k_2 = (x_2 P_2^+, 0, \mathbf{k}_{2T}), \quad k_3 = (0, x_3 P_3^-, \mathbf{k}_{3T}). \quad (19)$$

For these considered decay channels, the integration over $k_1^-, k_2^-,$ and k_3^+ in Eq.(16) will lead to

$$\mathcal{A}(B \rightarrow K^* a_0) \sim \int dx_1 dx_2 dx_3 b_1 db_1 b_2 db_2 b_3 db_3 \cdot \text{Tr} [C(t) \Phi_B(x_1, b_1) \Phi_{K^*}(x_2, b_2) \Phi_{a_0}(x_3, b_3) H(x_i, b_i, t) S_t(x_i) e^{-S(t)}], \quad (20)$$

where b_i is the conjugate space coordinate of k_{iT} , and t is the largest energy scale in function $H(x_i, b_i, t)$. In order to smear the end-point singularity on x_i , the jet function $S_t(x)$ [20], which comes from the resummation of the double logarithms $\ln^2 x_i$, is used. The last term $e^{-S(t)}$ in Eq.(20) is the Sudakov form factor which suppresses the soft dynamics effectively [21].

For the considered decays, the related weak effective Hamiltonian H_{eff} can be written as [22]

$$\mathcal{H}_{eff} = \frac{G_F}{\sqrt{2}} \left[\sum_{p=u,c} V_{pb} V_{ps}^* (C_1(\mu) O_1^p(\mu) + C_2(\mu) O_2^p(\mu)) - V_{tb} V_{ts}^* \sum_{i=3}^{10} C_i(\mu) O_i(\mu) \right], \quad (21)$$

where the Fermi constant $G_F = 1.16639 \times 10^{-5} \text{GeV}^{-2}$ and the functions $Q_i (i = 1, \dots, 10)$ are the local four-quark operators. We specify below the operators in \mathcal{H}_{eff} for $b \rightarrow s$ transition:

$$\begin{aligned} O_1^u &= \bar{s}_\alpha \gamma^\mu L u_\beta \cdot \bar{u}_\beta \gamma_\mu L b_\alpha, & O_2^u &= \bar{s}_\alpha \gamma^\mu L u_\alpha \cdot \bar{u}_\beta \gamma_\mu L b_\beta, \\ O_3 &= \bar{s}_\alpha \gamma^\mu L b_\alpha \cdot \sum_{q'} \bar{q}'_\beta \gamma_\mu L q'_\beta, & O_4 &= \bar{s}_\alpha \gamma^\mu L b_\beta \cdot \sum_{q'} \bar{q}'_\beta \gamma_\mu L q'_\alpha, \\ O_5 &= \bar{s}_\alpha \gamma^\mu L b_\alpha \cdot \sum_{q'} \bar{q}'_\beta \gamma_\mu R q'_\beta, & O_6 &= \bar{s}_\alpha \gamma^\mu L b_\beta \cdot \sum_{q'} \bar{q}'_\beta \gamma_\mu R q'_\alpha, \\ O_7 &= \frac{3}{2} \bar{s}_\alpha \gamma^\mu L b_\alpha \cdot \sum_{q'} e_{q'} \bar{q}'_\beta \gamma_\mu R q'_\beta, & O_8 &= \frac{3}{2} \bar{s}_\alpha \gamma^\mu L b_\beta \cdot \sum_{q'} e_{q'} \bar{q}'_\beta \gamma_\mu R q'_\alpha, \\ O_9 &= \frac{3}{2} \bar{s}_\alpha \gamma^\mu L b_\alpha \cdot \sum_{q'} e_{q'} \bar{q}'_\beta \gamma_\mu L q'_\beta, & O_{10} &= \frac{3}{2} \bar{s}_\alpha \gamma^\mu L b_\beta \cdot \sum_{q'} e_{q'} \bar{q}'_\beta \gamma_\mu L q'_\alpha, \end{aligned} \quad (22)$$

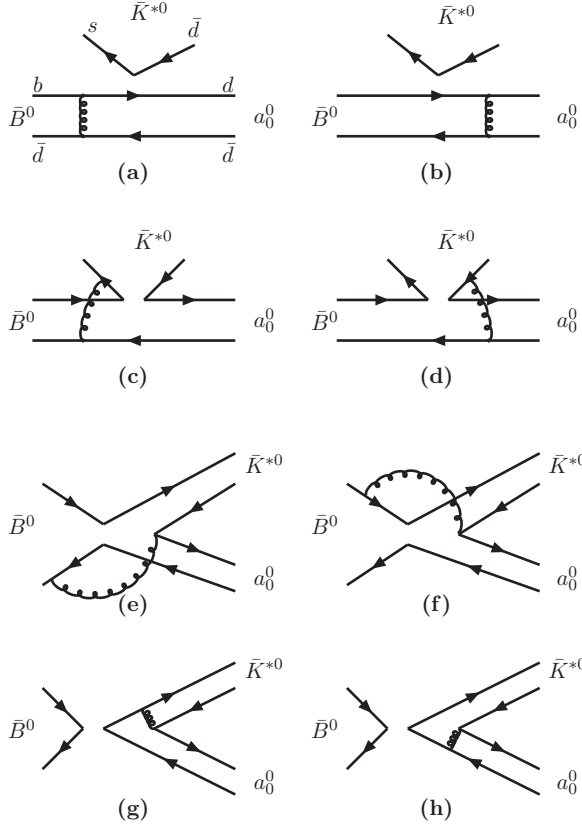


FIG. 1: Diagrams contributing to the decay $\bar{B}^0 \rightarrow \bar{K}^{*0} a_0^0(1450)$.

where α and β are the $SU(3)$ color indices; L and R are the left- and right-handed projection operators with $L = (1 - \gamma_5)$, $R = (1 + \gamma_5)$. The sum over q' runs over the quark fields that are active at the scale $\mu = O(m_b)$, i.e., $(q' \in \{u, d, s, c, b\})$.

In Fig. 1, we give the leading order Feynman diagrams for the channel $\bar{B}^0 \rightarrow a_0^0(1450)K^{*0}$ as an example. For the factorizable and nonfactorizable emission diagrams Fig.1(a), 1(b) and 1(c), 1(d), if one exchanges the K^{*0} and a_0^0 , the corresponding diagrams also exist. But there are not this kind of exchange diagrams for the factorizable and nonfactorizable annihilation diagrams, that is Fig.1 (e), 1(f) and 1(g), 1(h). If we replace the \bar{d} quark in both \bar{B}^0 and a_0^0 with \bar{u} quark, we will get the Feynman diagrams for the decay $B^- \rightarrow a_0^-(1450)K^{*0}$. If we replace the $d(\bar{d})$ quark in $a_0^0(K^{*0})$ with $u(\bar{u})$, we will get the Feynman diagrams for the decay $\bar{B}^0 \rightarrow a_0^+(1450)K^{*-}$. While there are not the diagrams obtained by exchanging the two final state mesons for these two channels. For the decay $B^- \rightarrow a_0^0(1450)K^{*-}$, its Feynman diagrams are distinctive: the meson $a_0(1450)$ is emitted (the upper meson) in the factorizable (nonfactorizable) emission diagrams, while the meson K^* is the upper meson in the factorizable (nonfactorizable) annihilation diagrams. The detailed analytic formulae for the diagrams of each decay are not presented and can be obtained from those of $B \rightarrow f_0(980)K^*$ [23] by replacing corresponding wave functions and parameters.

Combining the contributions from different diagrams, the total decay amplitudes for

these decays can be written as

$$\begin{aligned}\sqrt{2}\mathcal{M}(\bar{K}^{*0}a_0^0) &= \xi_u M_{eK^*} C_2 - \xi_t \left[M_{eK^*} \frac{3C_{10}}{2} + M_{eK^*}^{P2} \frac{3C_8}{2} - (F_{ea_0} + F_{aa_0}) \left(a_4 - \frac{a_{10}}{2} \right) \right. \\ &\quad - (M_{ea_0} + M_{aa_0}) \left(C_3 - \frac{1}{2}C_9 \right) - (M_{ea_0}^{P1} + M_{aa_0}^{P1}) \left(C_5 - \frac{1}{2}C_7 \right) \\ &\quad \left. - F_{aa_0}^{P2} \left(a_6 - \frac{1}{2}a_8 \right) \right],\end{aligned}\quad (23)$$

$$\begin{aligned}\mathcal{M}(\bar{K}^{*0}a_0^-) &= \xi_u [M_{aa_0} C_1 + F_{aa_0} a_1] - \xi_t \left[F_{ea_0} \left(a_4 - \frac{a_{10}}{2} \right) + F_{aa_0} (a_4 + a_{10}) \right. \\ &\quad + M_{ea_0} \left(C_3 - \frac{1}{2}C_9 \right) + M_{aa_0} (C_3 + C_9) + M_{ea_0}^{P1} \left(C_5 - \frac{1}{2}C_7 \right) \\ &\quad \left. + M_{aa_0}^{P1} (C_5 + C_7) + F_{aa_0}^{P2} (a_6 + a_8) \right],\end{aligned}\quad (24)$$

$$\begin{aligned}\sqrt{2}\mathcal{M}(\bar{K}^{*-}a_0^0) &= \xi_u [M_{eK^*} C_2 + M_{aa_0} C_1 + F_{aa_0} a_1] - \xi_t \left[M_{eK^*} \frac{3}{2}C_{10} + M_{eK^*}^{P2} \frac{3}{2}C_8 \right. \\ &\quad + M_{aa_0} (C_3 + C_9) + M_{aa_0}^{P1} (C_5 + C_7) \\ &\quad \left. + F_{aa_0} (a_4 + a_{10}) + F_{aa_0}^{P2} (a_6 + a_8) \right],\end{aligned}\quad (25)$$

$$\begin{aligned}\mathcal{M}(\bar{K}^{*-}a_0^+) &= \xi_u [F_{ea_0} a_1 + M_{ea_0} C_1] - \xi_t \left[F_{ea_0} (a_4 + a_{10}) + M_{ea_0} (C_3 + C_9) \right. \\ &\quad + M_{ea_0}^{P1} (C_5 + C_7) + M_{aa_0} \left(C_3 - \frac{1}{2}C_9 \right) + M_{aa_0}^{P1} \left(C_5 - \frac{1}{2}C_7 \right) \\ &\quad \left. + F_{aa_0} \left(a_4 - \frac{1}{2}a_{10} \right) + F_{aa_0}^{P2} \left(a_6 - \frac{1}{2}a_8 \right) \right],\end{aligned}\quad (26)$$

The combinations of the Wilson coefficients are defined as usual [24]:

$$\begin{aligned}a_1(\mu) &= C_2(\mu) + \frac{C_1(\mu)}{3}, & a_2(\mu) &= C_1(\mu) + \frac{C_2(\mu)}{3}, \\ a_i(\mu) &= C_i(\mu) + \frac{C_{i+1}(\mu)}{3}, & i &= 3, 5, 7, 9, \\ a_i(\mu) &= C_i(\mu) + \frac{C_{i-1}(\mu)}{3}, & i &= 4, 6, 8, 10.\end{aligned}\quad (27)$$

IV. NUMERICAL RESULTS AND DISCUSSIONS

We use the following input parameters in the numerical calculations [25, 26]:

$$f_B = 190 \text{ MeV}, M_B = 5.28 \text{ GeV}, M_W = 80.41 \text{ GeV}, \quad (28)$$

$$V_{ub} = |V_{ub}| e^{-i\gamma} = 3.93 \times 10^{-3} e^{-i68^\circ}, \quad (29)$$

$$V_{us} = 0.2255, V_{tb} = 1.0, V_{ts} = 0.0387, \quad (30)$$

$$\tau_{B^\pm} = 1.638 \times 10^{-12} \text{ s}, \tau_{B^0} = 1.530 \times 10^{-12} \text{ s}. \quad (31)$$

Using the wave functions and the values of relevant input parameters, we find the numerical values of the form factor $B \rightarrow a_0(1450)$ at zero momentum transfer:

$$F_0^{\bar{B}^0 \rightarrow a_0}(q^2 = 0) = -0.42_{-0.03-0.03-0.04-0.07}^{+0.04+0.04+0.05+0.06}, \quad \text{scenario I}, \quad (32)$$

$$F_0^{\bar{B}^0 \rightarrow a_0}(q^2 = 0) = 0.86_{-0.03-0.04-0.09-0.11}^{+0.04+0.05+0.10+0.14}, \quad \text{scenario II}, \quad (33)$$

where the uncertainties are mainly from the Gegenbauer moments B_1 , B_3 , the decay constant of the meson $a_0(1450)$, the B -meson shape parameter $\omega = 0.40 \pm 0.04$ GeV. These predictions are larger than those given in Ref.[27], for using different values for the threshold parameter c in the jet function. Certainly, they are consistent with each other in errors.

In the B -rest frame, the decay rates of $B \rightarrow a_0(1450)K^*$ can be written as

$$\Gamma = \frac{G_F^2}{32\pi m_B} |\mathcal{M}|^2 (1 - r_{a_0}^2), \quad (34)$$

where \mathcal{M} is the total decay amplitude of each considered decay and r_{a_0} the mass ratio, which have been given in Sec. III. \mathcal{M} can be rewritten as

$$\mathcal{M} = V_{ub}V_{us}^*T - V_{tb}V_{ts}^*P = V_{ub}V_{us}^* [1 + ze^{i(\delta-\gamma)}], \quad (35)$$

where γ is the Cabibbo-Kobayashi-Maskawa weak phase angle, and δ is the relative strong phase between the tree and the penguin amplitudes, which are denote as "T" and "P", respectively. The term z describes the ratio of penguin to tree contributions and is defined as

$$z = \left| \frac{V_{tb}V_{ts}^*}{V_{ub}V_{us}^*} \right| \left| \frac{P}{T} \right|. \quad (36)$$

From Eq.(35), it is easy to write decay amplitude $\overline{\mathcal{M}}$ for the corresponding conjugated decay mode. So the CP-averaged branching ratio for each considered decay is defined as

$$\mathcal{B} = (|\mathcal{M}|^2 + |\overline{\mathcal{M}}|^2)/2 = |V_{ub}V_{us}^*T|^2 [1 + 2z \cos \gamma \cos \delta + z^2]. \quad (37)$$

Using the input parameters and the wave functions as specified in this and previous sections, it is easy to get the branching ratios in two scenarios:

$$\mathcal{B}(B^- \rightarrow a_0^0(1450)K^{*-}) = (2.8_{-0.4-0.0-0.6-0.1}^{+0.4+1.0+0.6+0.1}) \times 10^{-6}, \textit{ScenarioI}, \quad (38)$$

$$\mathcal{B}(B^- \rightarrow a_0^-(1450)\bar{K}^{*0}) = (3.3_{-0.4-0.3-0.7-1.5}^{+0.6+0.4+0.8+2.7}) \times 10^{-6}, \textit{ScenarioI}, \quad (39)$$

$$\mathcal{B}(\bar{B}^0 \rightarrow a_0^+(1450)K^{*-}) = (3.6_{-0.6-0.1-0.7-1.1}^{+0.6+0.3+0.8+2.0}) \times 10^{-6}, \textit{ScenarioI}, \quad (40)$$

$$\mathcal{B}(\bar{B}^0 \rightarrow a_0^0(1450)\bar{K}^{*0}) = (1.2_{-0.1-0.2-0.3-0.6}^{+0.1+0.1+0.2+1.0}) \times 10^{-6}, \textit{ScenarioI}; \quad (41)$$

$$\mathcal{B}(B^- \rightarrow a_0^0(1450)K^{*-}) = (7.0_{-0.7-1.1-1.4-0.0}^{+0.9+1.6+1.7+0.2}) \times 10^{-6}, \textit{ScenarioII}, \quad (42)$$

$$\mathcal{B}(B^- \rightarrow a_0^-(1450)\bar{K}^{*0}) = (3.0_{-0.1-0.1-0.6-0.7}^{+0.2+0.2+0.7+1.2}) \times 10^{-5}, \textit{ScenarioII}, \quad (43)$$

$$\mathcal{B}(\bar{B}^0 \rightarrow a_0^+(1450)K^{*-}) = (2.8_{-0.3-0.0-0.5-0.6}^{+0.3+0.1+0.7+0.8}) \times 10^{-5}, \textit{ScenarioII}, \quad (44)$$

$$\mathcal{B}(\bar{B}^0 \rightarrow a_0^0(1450)\bar{K}^{*0}) = (1.4_{-0.1-0.1-0.3-0.4}^{+0.1+0.0+0.3+0.5}) \times 10^{-5}, \textit{ScenarioII}. \quad (45)$$

In the above results, the first two errors come from the uncertainties of the Gegenbauer moments B_1 , B_3 of the scalar meson, and the third one is from the decay constant of $a_0(1450)$. The last one comes from the uncertainty in the B meson shape parameter $\omega_b = 0.40 \pm 0.04$ GeV. We also show the dependence of the branching ratios for these considered decays on the Cabibbo-Kobayashi-Maskawa angle γ in Fig. 2 and Fig. 3.

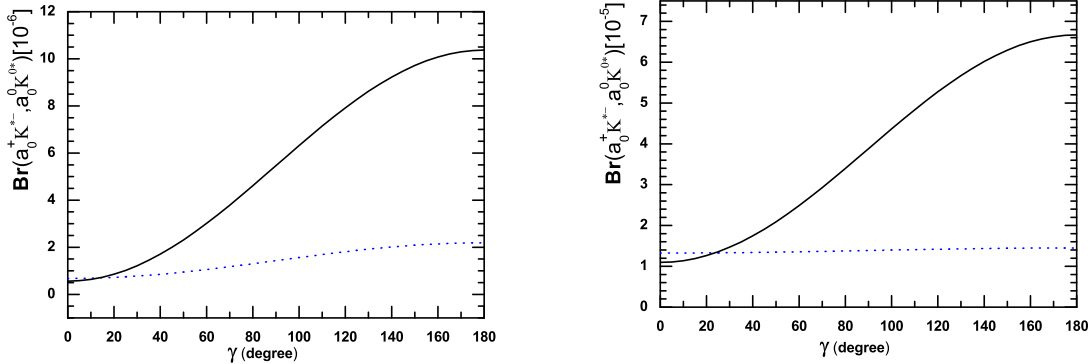


FIG. 2: The dependence of the branching ratios for $\bar{B}^0 \rightarrow a_0^+(1450)K^{*-}$ (solid curve) and $\bar{B}^0 \rightarrow a_0^0(1450)\bar{K}^{*0}$ (dotted curve) on the Cabibbo-Kobayashi-Maskawa angle γ . The left (right) panel is plotted in scenario I (II).

The branching ratios predicted by QCD factorization approach for these considered decays in scenario II are listed as [16]

$$\mathcal{B}(B^- \rightarrow a_0^0(1450)K^{*-}) = (2.2_{-4.0}^{+4.9+0.7+22.5}) \times 10^{-6}, \quad (46)$$

$$\mathcal{B}(B^- \rightarrow a_0^-(1450)\bar{K}^{*0}) = (7.8_{-11.0}^{+14.3+0.9+23.4}) \times 10^{-6}, \quad (47)$$

$$\mathcal{B}(\bar{B}^0 \rightarrow a_0^+(1450)K^{*-}) = (4.7_{-3.7}^{+4.4+1.0+14.6}) \times 10^{-6}, \quad (48)$$

$$\mathcal{B}(\bar{B}^0 \rightarrow a_0^0(1450)\bar{K}^{*0}) = (2.5_{-3.7}^{+4.4+1.0+14.6}) \times 10^{-6}. \quad (49)$$

Though it is well known that the annihilation diagram contributions to charmless hadronic B decays are power suppressed in the heavy-quark limit, as emphasized in [28], these contributions may be important for some B meson decays, here considered channels are just this kind of decays. For this kind decays, the factorizable annihilation diagrams almost guide the final branching ratios, so it is important to calculate correctly the amplitudes from these diagrams. While the annihilation amplitude has endpoint divergence even at twist-2 level in QCD factorization calculations, and one cannot compute it in a self-consistent way and has to parameterize phenomenologically the endpoint divergence. So it is difficult to avoid to bring many uncertainties to the final results. In fact, the major uncertainties listed in Eq.(46-49) are just from the contributions of annihilation diagrams. Comparing with QCD factorization approach, PQCD approach can make a reliable calculation from factorizable annihilation diagrams in k_T factorization [29]. The endpoint singularity occurred in QCD factorization approach is cured here by the Sudakov factor. Because of the large uncertainties from QCD factorization approach, our predictions in scenario II are also in agreement with the QCD factorization results within theoretical errors.

In Table I, we list the values of the factorizable and nonfactorizable amplitudes from the emission and annihilation topology diagrams of the considered decays in both scenarios. $F_e(a)a_0$ and $M_e(a)a_0$ are the K^* -meson emission (annihilation) factorizable contributions

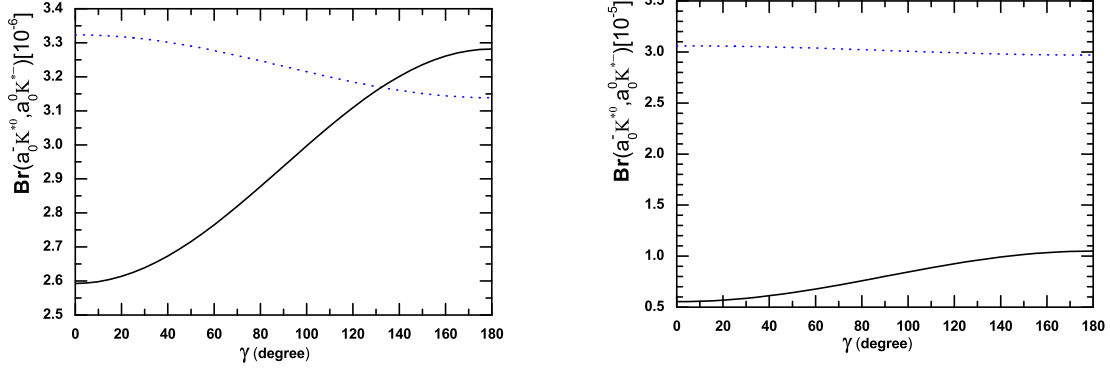


FIG. 3: The dependence of the branching ratios for $B^- \rightarrow a_0^0(1450)K^{*-}$ (solid curve) and $B^- \rightarrow a_0^-(1450)\bar{K}^{*0}$ (dotted curve) on the Cabibbo-Kobayashi-Maskawa angle γ . The left (right) panel is plotted in scenario I (II).

TABLE I: Decay amplitudes for decays $B^- \rightarrow a_0^0 K^{*-}, a_0^- \bar{K}^{*0}, \bar{B}^0 \rightarrow a_0^+ K^{*-}, a_0^0 \bar{K}^{*0}$ ($\times 10^{-2} \text{GeV}^3$) in the two scenarios.

| | $F_{ea_0}^T$ | F_{ea_0} | $M_{ea_0}^T + M_{eK^*}^T$ | $M_{ea_0} + M_{eK^*}$ | $M_{aa_0}^T$ | M_{aa_0} | $F_{aa_0}^T$ | F_{aa_0} |
|----------------------------|--------------|------------|---------------------------|-----------------------|---------------|-----------------|---------------|----------------|
| $a_0^0 K^{*-}$ (SI) | ... | ... | $-32.6 + 59.5i$ | $-0.14 + 0.30i$ | $-1.8 + 3.2i$ | $0.11 - 0.06i$ | $-0.5 - 3.5i$ | $5.3 + 1.5i$ |
| $a_0^- \bar{K}^{*0}$ (SI) | ... | -12.5 | ... | $-0.27 + 0.00i$ | $-2.5 + 4.5i$ | $0.16 - 0.08i$ | $-0.7 - 4.9i$ | $7.1 + 2.6i$ |
| $a_0^+ K^{*-}$ (SI) | 272.8 | -12.0 | $11.3 - 8.3i$ | $0.02 - 0.28i$ | ... | $0.20 - 0.19i$ | ... | $7.3 + 2.4i$ |
| $a_0^0 \bar{K}^{*0}$ (SI) | ... | 8.9 | $-32.6 + 59.5i$ | $0.07 + 0.31i$ | ... | $-0.14 + 0.13i$ | ... | $-5.2 - 1.9i$ |
| $a_0^0 K^{*-}$ (SII) | ... | ... | $47.9 + 39.0i$ | $0.23 + 0.18i$ | $6.7 + 1.6i$ | $-0.25 - 0.17i$ | $0.6 + 1.1i$ | $-5.2 - 7.9i$ |
| $a_0^- \bar{K}^{*0}$ (SII) | ... | 22.9 | ... | $-0.73 + 0.70i$ | $9.5 + 2.3i$ | $-0.36 - 0.25i$ | $1.0 + 1.5i$ | $-6.9 - 11.6i$ |
| $a_0^+ K^{*-}$ (SII) | -548.5 | 22.1 | $-1.5 - 6.4i$ | $-0.84 + 0.57i$ | ... | $-0.56 - 0.30i$ | ... | $-7.1 - 11.6i$ |
| $a_0^0 \bar{K}^{*0}$ (SII) | ... | -16.2 | $47.9 + 39.0i$ | $0.72 - 0.33i$ | ... | $0.40 + 0.21i$ | ... | $5.0 + 8.2i$ |

nonfactorizable contributions from penguin operators, respectively. The upper label T denotes the contributions from tree operators. For the decays $B^- \rightarrow a_0^0 K^{*-}$ and $\bar{B}^0 \rightarrow a_0^0 \bar{K}^{*0}$, there also exists the contributions from a_0 emission nonfactorizable diagrams.

In order to show the importance of the contributions from penguin operators, we can show the branching ratio in another way:

$$\mathcal{B} = |V_{ub}V_{us}^*|^2(T_r^2 + T_i^2) + |V_{tb}V_{ts}^*|^2(P_r^2 + P_i^2) - |V_{ub}V_{us}^*V_{tb}V_{ts}^*| \cos \gamma (T_r P_r + T_i P_i). \quad (50)$$

If the both sides of the upper equation are divided by the constant $|V_{ub}V_{us}^*|^2$, one can get

$$\begin{aligned} \frac{\mathcal{B}}{|V_{ub}V_{us}^*|^2} &= (T_r^2 + T_i^2) + \left| \frac{V_{tb}V_{ts}^*}{V_{ub}V_{us}^*} \right|^2 (P_r^2 + P_i^2) - \left| \frac{V_{tb}V_{ts}^*}{V_{ub}V_{us}^*} \right| \cos \gamma (T_r P_r + T_i P_i) \\ &= (T_r^2 + T_i^2) + 1936(P_r^2 + P_i^2) - 16.3(T_r P_r + T_i P_i). \end{aligned} \quad (51)$$

From Eq.(51), we can find the contributions from tree operators are strongly CKM-suppressed compared with those from penguin operators. Certainly, the contributions from the conference of tree and penguin operators are also small. So generally speaking, the branching ratios are proportional to $(P_r^2 + P_i^2)$, that is to say if ones penguin operator contributions are large, its branching ratio is also large. But the branching ratio of $\bar{B}^0 \rightarrow a_0^+(1450)K^{*-}$ for scenario I is excepted. It is because the contributions from tree operators are enhanced very much by the large Wilson coefficients $a_1 = C_2 + C_1/3$, which results they are very large to survive the aforementioned suppression. So exactly speaking, the mode $\bar{B}^0 \rightarrow a_0^+(1450)K^{*-}$ is a tree-dominated decay in scenario I. On the other side, the conferences from tree and penguin operators also strengthen the final result. So, even though the contributions from the penguin operators for this channel are the smallest in scenario I, instead, it receives a larger branching ratio. Another abnormal decay channel is $B^- \rightarrow a_0^0(1450)K^{*-}$. In scenario II, the branching ratios of other three decays are at the order of 10^{-5} , while the branching ratio of decay $B^- \rightarrow a_0^0(1450)K^{*-}$ is the smallest one and only a few times 10^{-6} . The reason is that the contributions from penguin operators of this decay are the smallest. Compared with the decay $B^- \rightarrow a_0^-(1450)\bar{K}^{*0}$ though, the decay mode $a_0^0(1450)K^{*-}$ receives extra tree contributions $M_{eK^*}^T + M_{eK^*}^T$, which makes its total tree contribution almost 7 times larger than that of the mode $a_0^-(1450)\bar{K}^{*0}$, while as mentioned above, the tree contributions are strongly suppressed and not much helpful to enhance the branching ratio. Compared with other three decays, the decay $B^- \rightarrow a_0^0(1450)K^{*-}$ does not receive the enhancement from the K^* -emission factorizable diagrams and get the smallest contributions from the penguin operators, which makes its branching ratio curve shown in Fig. 3 drop a lot. Certainly, the mode $a_0^0(1450)K^{*-}$ does not receive this kind of enhancement (that is F_{ea_0}) in scenario I, too. In fact, F_{ea_0} and F_{aa_0} shown in Table I are destructive for the other three decays in both scenarios. The destruction induces the mode $a_0^0\bar{K}^{*0}$ receives a smaller penguin amplitude compared with the mode $a_0^0(1450)K^{*-}$ in scenario I.

Now we turn to the evaluations of the direct CP-violating asymmetries of the considered decays in PQCD approach. The direct CP-violating asymmetry can be defined as

$$\mathcal{A}_{CP}^{dir} = \frac{|\overline{\mathcal{M}}|^2 - |\mathcal{M}|^2}{|\mathcal{M}|^2 + |\overline{\mathcal{M}}|^2} = \frac{2z \sin \gamma \sin \delta}{1 + 2z \cos \gamma \cos \delta + z^2}. \quad (52)$$

Using the input parameters and the wave functions as specified in this and previous sections, one can find the PQCD predictions (in units of 10^{-2}) for the direct CP-violating

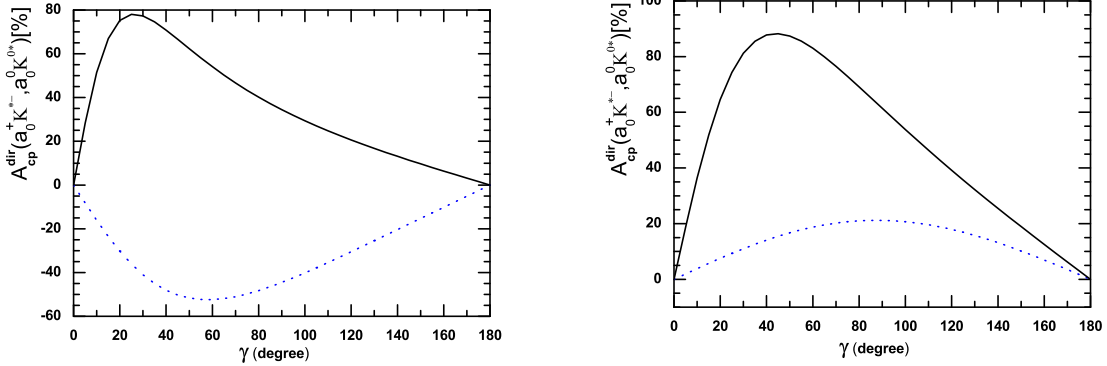


FIG. 4: Direct CP-violating asymmetries of $\bar{B}^0 \rightarrow a_0^+(1450)K^{*-}$ (solid curve) and $\bar{B}^0 \rightarrow a_0^0(1450)\bar{K}^{*0}$ (dotted curve), as functions of the Cabibbo-Kobayashi-Maskawa angle γ . The left (right) panel is plotted in scenario I (II).

asymmetries of the considered decays

$$\mathcal{A}_{CP}^{dir}(B^- \rightarrow a_0^0(1450)K^{*-}) = -50.1_{-8.8-0.0-0.0-0.6}^{+8.4+4.7+0.5+2.6}, \text{ scenario I,} \quad (53)$$

$$\mathcal{A}_{CP}^{dir}(B^- \rightarrow a_0^-(1450)\bar{K}^{*0}) = 2.0_{-0.8-0.0-0.0-0.1}^{+1.5+0.4+0.2+0.8}, \text{ scenario I,} \quad (54)$$

$$\mathcal{A}_{CP}^{dir}(\bar{B}^0 \rightarrow a_0^+(1450)K^{*-}) = 48.0_{-20.5-6.1-0.0-12.8}^{+19.2+1.5+0.1+13.5}, \text{ scenario I,} \quad (55)$$

$$\mathcal{A}_{CP}^{dir}(\bar{B}^0 \rightarrow a_0^0(1450)\bar{K}^{*0}) = -50.8_{-20.5-0.1-0.6-11.9}^{+20.2+0.1+0.0+12.7}, \text{ scenario I,} \quad (56)$$

$$\mathcal{A}_{CP}^{dir}(B^- \rightarrow a_0^0(1450)K^{*-}) = -11.4_{-1.7-0.3-0.0-1.1}^{+1.5+0.3+0.1+2.0}, \text{ scenario II,} \quad (57)$$

$$\mathcal{A}_{CP}^{dir}(B^- \rightarrow a_0^-(1450)\bar{K}^{*0}) = -1.8_{-0.2-0.1-0.0-0.2}^{+0.3+0.2+0.0+0.2}, \text{ scenario II,} \quad (58)$$

$$\mathcal{A}_{CP}^{dir}(\bar{B}^0 \rightarrow a_0^+(1450)K^{*-}) = 78.0_{-2.5-5.4-0.1-8.8}^{+2.2+4.8+0.0+6.6}, \text{ scenario II,} \quad (59)$$

$$\mathcal{A}_{CP}^{dir}(\bar{B}^0 \rightarrow a_0^0(1450)\bar{K}^{*0}) = 20.0_{-3.1-1.7-0.0-1.3}^{+2.5+1.7+0.0+0.8}, \text{ scenario II.} \quad (60)$$

The main errors are induced by the uncertainties of B_1 and B_3 of $a_0(1450)$, f_{a_0} and B meson shape parameter ω_b .

The direct CP-violating asymmetries of these considered decays are displayed in Fig. 4 and Fig. 5. From these figures, one can find the direct CP-violating asymmetries of the decays $\bar{B}^0 \rightarrow a_0^+(1450)K^{*-}$ and $B^- \rightarrow a_0^0(1450)K^{*-}$ have the same sign in the two scenarios, while those of the decays $B^- \rightarrow a_0^-(1450)\bar{K}^{*0}$ and $\bar{B}^0 \rightarrow a_0^0(1450)\bar{K}^{*0}$ have contrary signs in the two scenarios. If the value of z [defined in Eq.(35)] is very large, for example, $z_{a_0^-\bar{K}^{*0}} = 91.1$ (scenario I) and 78.8 (scenario II), the corresponding direct CP-violating asymmetry will be very small and only a few percent. If the value of z is small and only a few, for example, $z_{a_0^0K^{*-}} = 6.2$ (scenario II) and $z_{a_0^0\bar{K}^{*0}} = 9.2$ (scenario II), the corresponding direct CP-violating asymmetry is large. If the value of z is very small and not far away from 1, then this condition is complex, for the direct CP-violating asymmetry is very sensitive to the relative strong phase angle δ , for example, $z_{a_0^+K^{*-}} = 0.88$ (scenario I) and $z_{a_0^+K^{*-}} = 1.32$ (scenario II), though these two values are close to each other, but their corresponding direct CP-violating asymmetries are very different.

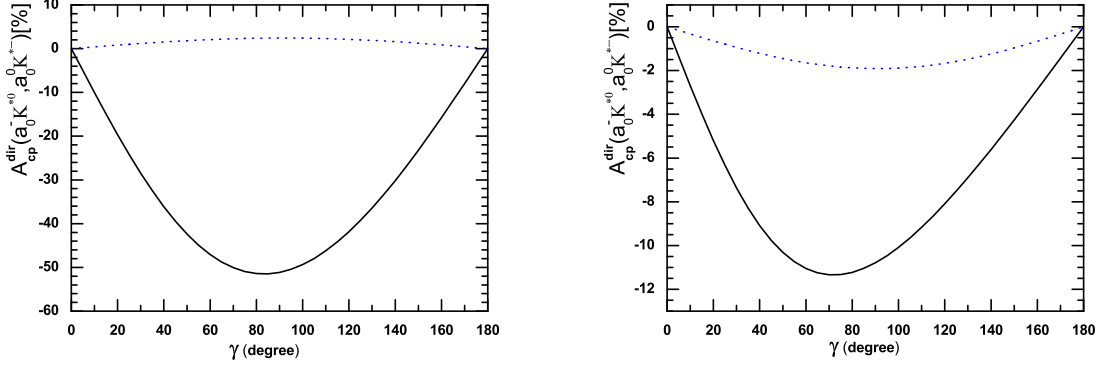


FIG. 5: Direct CP-violating asymmetries of $B^- \rightarrow a_0^0(1450)K^{*-}$ (solid curve) and $B^- \rightarrow a_0^-(1450)\bar{K}^{*0}$ (dotted curve) as functions of the Cabibbo-Kobayashi-Maskawa angle γ . The left (right) panel is plotted in scenario I (II).

In order to characterize the symmetry breaking effects and the contribution from tree operators and the electro-weak penguin, it is useful to define the parameters below:

$$R_1 = \frac{\mathcal{B}(\bar{B}^0 \rightarrow a_0^0(1450)\bar{K}^{*0})}{\mathcal{B}(\bar{B}^0 \rightarrow a_0^+(1450)K^{*-})}, \quad (61)$$

$$R_2 = \frac{\mathcal{B}(B^- \rightarrow a_0^0(1450)K^{*-})}{\mathcal{B}(B^- \rightarrow a_0^-(1450)\bar{K}^{*0})}, \quad (62)$$

$$R_3 = \frac{\tau(B^0) \mathcal{B}(B^- \rightarrow a_0^-(1450)\bar{K}^{*0})}{\tau(B^-) \mathcal{B}(\bar{B}^0 \rightarrow a_0^+(1450)K^{*-})}. \quad (63)$$

Considering the ratios of the branching ratios is a more transparent comparison between the predictions and the data because they are less sensitive to the nonperturbative inputs. So the large deviation of these ratios from the standard-model predictions could reveal a signal of new physics. When we ignore the tree diagrams and electro-weak penguins, R_1, R_2 , and R_3 should be equal to 0.5, 0.5, and 1.0. From our calculations, their values are:

$$R_1 = 0.33, R_2 = 0.85, R_3 = 0.86, \text{ scenario I}, \quad (64)$$

$$R_1 = 0.50, R_2 = 0.23, R_3 = 1.00, \text{ scenario II}. \quad (65)$$

One can find the ratios R_1 and R_3 for scenario II are in agreement well with the predictions, while there is a large deviation for the ratio R_2 , and the reason is the aforementioned smallest penguin operator contributions for the channel $B^- \rightarrow a_0^0(1450)K^{*-}$. For scenario I, there are large deviation for all three ratios and the deviation for R_2 is the largest. These ratios can be tested by the future experiments.

V. CONCLUSION

In this paper, by using the decay constants and light-cone distribution amplitudes derived from QCD sum-rule method, we calculate the branching ratios and the direct CP-violating asymmetries of decays $B \rightarrow a_0(1450)K^*$ in the PQCD factorization approach and find that

- For the decays $B^- \rightarrow a_0^-(1450)K^{*0}$, $\bar{B}^0 \rightarrow a_0^+(1450)K^{*-}$, $a_0^0(1450)\bar{K}^{*0}$, their branching ratios in scenario II are larger than those in scenario I about one order. So it is easy for the experiments to differentiate between the lowest lying state and the first excited state for the meson $a_0(1450)$.
- For the decay $B^- \rightarrow a_0^0(1450)K^{*-}$, due to not receiving the enhancement from the K^* -emission factorizable diagrams, its penguin operator contributions are the smallest in scenario II, which makes its branching ratio drop into the order of 10^{-6} , even so, its branching ratio in scenario II is still larger than that in scenario I about 2.5 times.
- The PQCD predictions are much larger than QCD factorization results. Because the latter can not make a reliable calculation from factorizable annihilation diagrams and bring large uncertainties into the branching ratios, so they are still consistent with each other within the large theoretical errors.
- For these considered decays, their tree contributions are strongly CKM suppressed and they are penguin dominant decay modes. But the decay $\bar{B}^0 \rightarrow a_0^+(1450)K^{*-}$ is abnormal in scenario I, for it receives an enhancement from the large Wilson coefficients $a_1 = C_2 + C_1/3$, which makes its tree contribution survive the suppression.
- The direct CP-violating asymmetry is determined by the ratio of penguin to tree contributions, that is z . Generally speaking, if the value of z is large, the corresponding direct CP-violating asymmetry will be small, vice versa. While if the value of z is very small and close to 1, the direct CP-violating asymmetry will be sensitive to the relative strong phase angle δ .

Acknowledgment

This work is partly supported by the National Natural Science Foundation of China under Grant No. 11047158, and by Foundation of Henan University of Technology under Grant No.150374.

-
- [1] N.A. Tornqvist, Phys. Rev. Lett. **49**, 624 (1982).
[2] G.L. Jaffe Phys. Rev. D **15**, 267 (1977); Erratum-ibid.Phys. Rev. D **15** 281 (1977);
A.L. Kataev, Phys. Atom. Nucl. **68**, 567 (2005), Yad. Fiz. 68, 597(2005); A. Vijande,
A. Valcarce, F. Fernandez and B. Silvestre-Brac, Phys. Rev. D**72**, 034025 (2005).

- [3] J. Weinstein , N. Isgur , Phys. Rev. Lett. **48**, 659 (1982); Phys. Rev. D **27**, 588 (1983); **41**, 2236 (1990); M.P. Locher et al., Eur. Phys. J. C **4**, 317 (1998).
- [4] V. Baru et al., Phys. Lett. B**586**, 53 (2004).
- [5] L. Celenza, et al., Phys. Rev. C **61**, 035201 (2000) .
- [6] M. Strohmeier-Presiccek, et al., Phys. Rev. D **60**, 054010 (1999) .
- [7] F.E. Close, A. Kirk, Phys. Lett. B **483** 345 (2000).
- [8] C.Amsler and F.E. Close, Phys. Lett. B **353**, 385 (1995); Phys. Rev. D **53**, 295 (1996).
- [9] F.E. Close, Q. Zhao, Phys. Rev. D **71**, 094022 (2005).
- [10] X.G. He, X.Q. Li, X. Liu, and X.Q. Zeng, Phys. Rev. D **73**, 051502 (2006).
- [11] H.Y. Cheng, C.K. Chua, K.F. Liu, Phys. Rev. D **74**, 094005 (2006).
- [12] W.M. Yao et al., (Particle Data Group), J.Phys. G **33**, 1 (2006).
- [13] N. Mathur, et al., Phys. Rev. D **76**, 114505, 2007.
- [14] L.J. Lee and D. Weingarten, Phys. Rev. D **61**, 014015 (2000); M. Gockeler et al., Phys. Rev. D **57**, 5562 (1998); S. Kim and S. Ohta, Nucl. Phts. Proc. Suppl. B **53**, 199 (1997); A. Hart, C. Mcneile, and C. Michael, Nucl. Phys. Proc. Suppl. B **119**, 266 (2003); T. Burch et al., Phys. Rev. D **73**, 094505 (2006).
- [15] W.A. Bardeen et al., Phys. Rev. D **65**, 014509 (2002); T. Kunihiro et. al, Phys. Rev. D **70**, 034504 (2004); S. Prelovsek et al., Phys. Rev. D **70**, 094503 (2004).
- [16] H.Y. Cheng, C.K. Chua and K.C. Yang, Phys. Rev. D **77**, 014034 (2008).
- [17] C.D. Lu and M.Z. Yang, Eur. Phys. J. C **28**, 515 (2003).
- [18] H.Y. Cheng , C.K. Chua , K.C. Yang Phys. Rev. D **73**, 014017 (2006).
- [19] P. Ball, G. W. Jones and R. Zwicky, Phys. Rev. D **75**, 054004 (2007).
- [20] H.N. Li, Phys. Rev. D **66**, 094010 (2002).
- [21] H.N. Li and B. Tseng, Phys. Rev. D **57**, 443 (1998).
- [22] G. Buchalla , A.J. Buras , M.E. Lautenbacher, Rev. Mod. Phys. **68**, 1125 (1996).
- [23] Z.Q. Zhang, J.D. Zhang, Eur. Phys. J. C **67**, 163 (2010).
- [24] Z.J. Xiao, Z.Q. Zhang, X. Liu, L.B. Guo, Phys. Rev. D **78**, 114001 (2008).
- [25] Particle Data Group, C. Amsler *et al.*, Phys. Lett. B **667**, 1 (2008).
- [26] BaBar Collaboration, P. del Amo Sanchez, *et al.*, arXiv:hep-ex/1005.1096.
- [27] R.H. Li, C.D. Lu, W. Wang, X.X. Wang, Phys. Rev. D **79**, 014013 (2009).
- [28] Y.Y. Keum, H.N. Li, A.I. Sanda, Phys. Rev. D **63**, 054008 (2001); Y.Y. Keum, H.N. Li, Phys. Rev. D **63**, 0754006 (2001).
- [29] X.Q. Yu, Y. Li, C.D. Lu, Phys. Rev.D **73**, 017501 (2006).